DALTON
FULL PAPER

The carbonylation of methanol catalysed by $[RhI(CO)(PEt_3)_2]$; crystal and molecular structure of $[RhMeI_2(CO)(PEt_3)_2]$†

Joanne Rankin,[a] Attila C. Benyei,[a] Andrew D. Poole[b] and David J. Cole-Hamilton*[a]

[a] *School of Chemistry, University of St. Andrews, St. Andrews, Fife, Scotland, UK KY16 9ST. E-mail: djc@st-and.ac.uk*
[b] *BP Amoco Chemicals, Salt End, Hull, UK HU12 8DS*

Received 1st July 1999, Accepted 13th September 1999

$[RhCl(CO)(PEt_3)_2]$ catalyses the carbonylation of methanol in the presence of MeI and water at a rate 1.8 times that for $[RhI_2(CO)_2]^-$ at 150 °C. The reaction is first order in [MeI] and zero order in p_{CO}. However, the phosphine complex degrades to $[Rh(CO)_2I_2]^-$ during the course of the reaction. Stoichiometric studies show that the rate of oxidative addition of MeI to $[RhI(CO)(PEt_3)_2]$ is 57 times faster than to $[RhI_2(CO)_2]^-$ at 298 K and that $[RhMeI_2(CO)(PEt_3)_2]$ can be isolated and crystallographically characterised. Combination of the methyl and carbonyl ligands to give the acyl intermediate occurs 38 times slower for $[RhMeI_2(CO)(PEt_3)_2]$ than for $[RhMeI_3(CO)_2]^-$ but the steady state concentration of the intermediates is different in that $[Rh(COMe)I_2(PEt_3)_2]$ is thermodynamically less stable than $[RhMeI_2(CO)(PEt_3)_2]$. In CH_2Cl_2, $[Rh(COMe)I_2(CO)(PEt_3)_2]$ reductively eliminates MeCOI. $[RhI(CO)(PEt_3)_2]$ reacts with CO to give $[RhI(CO)_2(PEt_3)_2]$. Catalyst degradation occurs *via* $[RhHI_2(CO)(PEt_3)_2]$, formed by oxidative addition of HI to $[RhI(CO)(PEt_3)_2]$, which reacts further with HI to give $[RhI_3(CO)(PEt_3)_2]$ from which $[Et_3PI]^+$ reductively eliminates and is hydrolysed to give Et_3PO. In the presence of water, much less $[RhI_3(CO)(PEt_3)_2]$ and Et_3PO are formed so the catalyst is more stable, but loss of $[Et_3PMe]^+$ and $[Et_3PH]^+$ from $[RhMeI_2(CO)(PEt_3)_2]$ or $[RhHI_2(CO)(PEt_3)_2]$, respectively, lead to catalyst deactivation. The rate determining step of the catalytic reaction in the presence of water is MeI oxidative addition to $[RhI(CO)(PEt_3)_2]$, but in the absence of water there is evidence that it may be reductive elimination of MeCOI from $[Rh(COMe)I_2(CO)(PEt_3)_2]$. $[RhMeI_2(CO)(PEt_3)_2]$ has mutually *trans* phosphines and the methyl group *trans* to I.

Introduction

Ethanoic acid is an important commodity chemical, much of which is produced commercially using methanol carbonylation using rhodium[1] or, more recently, iridium based catalysts.[2] Rhodium systems generally form $[Rh(CO)_2I_2]^-$ in solution and it is the high electron density on this anion which is generally considered to be responsible for the very high activity and selectivity of the catalyst.[3,4] Oxidative addition of iodomethane to this complex is 10^5 times faster than to comparable neutral species but is still the rate determining step for the overall methanol carbonylation reaction. Not only does this account for the higher rate of the reaction, but it also explains the high selectivity, since all metal containing intermediates in the reaction have a very short lifetime and hence are not susceptible to reactions such as hydrogenation, hydrogenolysis or reductive elimination of I_2 which might lead to side products such as methane, ethanal, ethanol, propanoic acid or propan-2-one.[1,3,4]

We have carried out extensive studies on the use of electron rich rhodium complexes,[5–9] particularly those in which the electron density is increased by the use of trialkylphosphine ligands. We reasoned that these complexes, being electron rich, might also be active for methanol carbonylation, particularly as $[RhI(CO)(PEt_3)_2]$ (ν_{CO} 1961 cm^{-1})[10] apparently has a higher electron density on the rhodium atom, as indicated by the degree of back-bonding into the π* orbitals of CO, than does $[Rh(CO)_2I_2]^-$ (ν_{CO} 2058, 1993 cm^{-1}).

Phosphine complexes of rhodium have been shown in the past[11–29] to be active for methanol carbonylation, sometimes at rates higher than those obtained under the same conditions with $[Rh(CO)_2I_2]^-$,[13,14,16,18] but there has been no other report of the use of alkyl phosphines in these reactions except that tetraalkyldiphosphine rhodium complexes are inactive.[17] Little information is available on the stability or degradation reactions of the catalysts. We now report a detailed study of the carbonylation of methanol using $[RhI(CO)(PEt_3)_2]$ as catalyst, as well as of the processes that lead to catalyst degradation. A preliminary report of some of these results has appeared.[30]

Experimental

Microanalyses were by the University of St. Andrews microanalytical service. NMR spectra were recorded from samples dissolved in CD_2Cl_2, C_6D_6 or CD_3OD on a Bruker AM 300 or a Varian 300 NMR spectrometer. The ^1H and ^{13}C NMR spectra were recorded with reference to tetramethylsilane (external). ^{31}P NMR spectra were referenced externally to 85% H_3PO_4. ^{13}C and ^{31}P NMR spectra were recorded with broad band proton decoupling. IR spectra were recorded using either a Perkin-Elmer 1710 or a Nicolet 460 Protege FTIR spectrometer. Atomic absorption analyses were carried out using a Philips PU 9400X atomic absorption spectrometer. Unless otherwise stated, analysis by gas chromatography (GC) was carried out using a Philips PU 4500 GC with a 25 m SGE BP1 column (100% dimethylsiloxane) and Chrompac software. The carrier gas was nitrogen (30 bar) and the temperature programme was 23 °C for 15 min. Gas chromatography–mass spectrometry (GC–MS) analysis was carried out using helium as a carrier gas with a Hewlett-Packard 5890 GC fitted with an Incos 50 electric quadrupole mass spectrometer. A 25 m SGE BP1 column was used.

All manipulations were performed using standard Schlenk line and catheter tubing techniques under nitrogen purified by passing through a glass column containing Cr(II) absorbed onto silica. All solvents were freshly distilled and dried; light petrol-

† *Supplementary data available*: rotatable 3-D crystal structure diagram in CHIME format. See http://www.rsc.org/suppdata/dt/1999/3771/

eum (bp 40–60 °C) and diethyl ether were distilled over sodium diphenylketyl and dichloromethane was distilled over calcium hydride. Ethanol and methanol were distilled over magnesium ethoxide or magnesium methoxide, respectively. Propanone was dried by refluxing over K_2CO_3 for 1 h. The following compounds were used as supplied without further purification: iodomethane, CD_3I, lithium iodide, anhydrous lithium iodide and sodium iodide (Aldrich); aqueous hydrogen chloride (11.6 mol dm^{-3}), aqueous hydrogen bromide (8.8 mol dm^{-3}) and aqueous hydrogen iodide (7.6 mol dm^{-3}) (Fisons); triethylphosphine (Strem); CD_2Cl_2, C_6D_6 and CD_3OD (Cambridge Isotope Laboratories). Ethanoic acid was used as supplied from BP Amoco Chemicals A5 plant or Prolabo. Methyl ethanoate (Aldrich) was distilled prior to use. $[RhCl(CO)_2]_2$ was used as supplied from Aldrich and was stored at 3 °C. $RhCl_3{\cdot}3H_2O$ was used as supplied from Avocado and was stored in a desiccator containing silica gel. Carbon monoxide was used as supplied from the British Oxygen Company. $Rh_2(OAc)_4{\cdot}2MeOH$,[31] $[RhX(CO)(PEt_3)_2]$ (X = Cl,[10] I[10] or OAc[7]) $[RhI(CO)_2]_2$[31] and $NBu_4[RhI_2(CO)_2]$.[31] were prepared by standard literature procedures.

Carbonyldiiodo(methyl)bis(triethylphosphine)rhodium(III)

Iodomethane (1 cm^3, 0.016 mol) was added to a Schlenk tube containing $[RhI(CO)(PEt_3)_2]$ (0.54 g, 1.09×10^{-3} mol). The orange mixture was stirred for 16 h before the excess iodomethane was removed *in vacuo*. Recrystallisation of the resulting orange solid from warm diethyl ether at 5 °C produced orange–yellow crystals of $[RhMeI_2(CO)(PEt_3)_2]$. Yield *ca.* 90%. NMR (CD_2Cl_2): ^{31}P, δ 2.4 (d, $^1J_{RhP} = 85.5$ Hz); ^{13}C, δ 183.3 (dt, $^1J_{CRh} = 63.6$, $^2J_{CP} = 9.8$, RhCO), 20.0 (t, $^1J_{CP} + {}^3J_{CP'} = 15.1$, PCH_2CH_3), 9.6 (s, PCH_2CH_3), −3.1 (dt, $^1J_{CRh} = 18.6$, $^2J_{CP} = 4.4$ Hz, $RhCH_3$); ^1H, δ 2.3 (12H, m, PCH_2CH_3), 1.2 (18H, m, PCH_2CH_3), 1.2‡ (3H, m, $RhCH_3$); ν_{CO} 2043 cm^{-1} (Found: C, 26.83, H, 5.37. $C_{14}H_{33}I_2OP_2Rh$ requires C, 26.44; H, 5.22%).

Carbonylhydridodiiodobis(triethylphosphine)rhodium(III)

An aqueous solution of HI (57% w/w, 0.11 cm^3, 0.10 g HI) was added to $[RhI(CO)(PEt_3)_2]$ (0.40 g, 8.06×10^{-4} mol) in propanone (30 cm^3). The mixture was stirred for 16 h before the liquid was removed *in vacuo*. The resulting yellow solid was crystallised from diethyl ether at 5 °C to produce yellow needles of $[RhHI_2(CO)(PEt_3)_2]$. Yield *ca.* 85%. NMR (CD_2Cl_2): ^{31}P, δ 13.2 (d, $^1J_{RhP} = 81.5$ Hz); ^{13}C, δ 182.0 (dt, $^1J_{CRh} = 63.4$, $^2J_{CP} = 10.1$, RhCO), 21.1 (t, $^1J_{CP} + {}^3J_{CP'} = 16.1$, PCH_2CH_3), 9.4 (s, PCH_2CH_3); ^1H, δ 2.3 (12H, m, PCH_2CH_3), 1.2 (18H, m, PCH_2CH_3), −11.1 (1H, dt, $^1J_{HRh} = 16.0$, $^2J_{HP} = 9.7$ Hz, RhH); ν_{CO} 2036 cm^{-1}, ν(Rh–H) = 1991 cm^{-1} (tentative assignment) (Found: C, 25.37; H, 4.85. $C_{13}H_{31}I_2OP_2Rh$ requires C, 25.10, H, 5.02%).

Attempted synthesis of carbonyldiiodoethanoylbis(triethylphosphine)rhodium(III)

Oxidative addition of ethanoyl chloride to $[RhI(CO)(PEt_3)_2]$. Ethanoyl chloride (1 cm^3, 0.014 mol) was added to $[RhI(CO)(PEt_3)_2]$, (0.39 g, 7.89×10^{-4} mol) in a Schlenk tube and the resulting orange–brown liquid was stirred for 16 h. The excess ethanoyl chloride was removed *in vacuo* to generate a yellow solid. Sodium iodide (0.60 g, 4.00×10^{-3} mol) and propan-2-one (10 cm^3) were added to the yellow solid and the solution was stirred for 2 h. The mixture was reduced to a small volume (*ca.* 1 cm^3) *in vacuo* and light petroleum was added to precipitate sodium salts. The salts were removed by filtration and propan-2-one was removed *in vacuo*.

‡ Obscured in the ^1H NMR spectrum but identified in the ^2H NMR spectrum of $[Rh(CD_3)I_2(CO)(PEt_3)_2]$, prepared from $[RhI(CO)(PEt_3)_2]$ and CD_3I.

Reaction of CO with $[RhMeI_2(CO)(PEt_3)_2]$. A solution of $[RhMeI_2(CO)(PEt_3)_2]$, (0.50 g, 7.86×10^{-4} mol) in CD_2Cl_2 was transferred to an autoclave which was pressurised with carbon monoxide (40 bar) and stirred for 16 h. After depressurising, the solution was transferred from the autoclave to a deoxygenated Schlenk tube by nitrogen pressure before the solvent was removed *in vacuo*. NMR: ^{31}P (CD_2Cl_2), δ 2.1 (d, $^1J_{RhP} = 88.2$ Hz); $^{13}C(C_6D_6)$ δ 226.4 (dt, $^1J_{CRh} = 25.0$, $^2J_{CP} = 4.6$, Rh*C*OCH$_3$), 179.3 (dt, $^1J_{CRh} = 69.1$, $^2J_{CP} = 7.6$, RhCO), 47.9 (d, $^1J_{CRh} = 3.1$, RhCO*C*H$_3$), 21.1 (t, $^1J_{CP} + {}^3J_{CP'} = 15.0$ Hz, P*C*H$_2$CH$_3$), 9.4 (s, PCH$_2$*C*H$_3$); $^1H(C_6D_6)$, δ 2.9 (3H, s, RhCOC*H$_3$*), 2.3 (12H, m, PC*H$_2$*CH$_3$), 1.0 (18H, m, PCH$_2$C*H$_3$*); $\nu_{CO} = 2065$ cm^{-1} (RhCO); $\nu_{CO} = 1665$ cm^{-1} (Rh*CO*CH$_3$).

Triethylmethylphosphium iodide, $[Et_3PMe]I$

A solution of triethylphosphine (100×10^{-6} dm^3, 6.7×10^{-4} mol) in diethyl ether (30 cm^3) was placed in a Schlenk flask. Iodomethane (42×10^{-6} dm^3, 6.7×10^{-4} mol) was added slowly and with stirring. The solution was allowed to stir for 15 min and diethyl ether was removed *in vacuo*.

Catalytic reactions

Batch catalytic reactions. These experiments were carried out inside glass liners within 250 cm^3 stainless steel autoclaves. The catalyst or catalyst precursor, (1.70×10^{-5}–8.0×10^{-5} mol) which was $[Rh(OAc)(CO)(PEt_3)_2]$, $[RhI(CO)(PEt_3)_2]$, or $[RhCl(CO)(PEt_3)_2]$, was dissolved in ethanol (4 cm^3, 0.068 mol) or methanol (4 cm^3, 0.099 mol) in a Schlenk tube. The air stable catalyst precursor $[Rh_2(OAc)_4]{\cdot}2MeOH$ was added directly to the autoclave when this was used as a rhodium source. In reactions which were carried out in the absence of a proton source, methyl ethanoate (4 cm^3, 0.050 mol) was used instead of methanol or ethanol. Other reagents were also added to the Schlenk tube.

A magnetic follower was added to the glass liner inside the autoclave. The autoclave was sealed and degassed by subjecting it to vacuum and nitrogen alternately three times. Iodomethane (1 cm^3, 0.016 mol) was added to the Schlenk tube just prior to transferring the reaction solution to the autoclave. In some reactions aqueous hydrogen chloride, aqueous hydrogen iodide or aqueous hydrogen bromide (1 cm^3, 5.83×10^{-3} mol) was added instead of iodomethane. By using the autoclave in a similar manner to a large Schlenk tube under an inert atmosphere, the reaction solution previously prepared was transferred to the autoclave.

The injection port was sealed and the autoclave was gently pressurised with carbon monoxide over 3 min (20–40 bar). A heating collar was used to heat the autoclave to the required temperature (80–185 °C) at a rate of 10 °C min^{-1} and a magnetic stirrer was used to stir the contents of the autoclave at 1000 rpm. After the heating period of between 1 and 4 h the autoclave was transferred to a cold water bath. Once cooled (*ca.* 45 min), the autoclave was slowly depressurised. The reaction solution was removed from the autoclave and transferred into a vial for analysis by GC or GC–MS. Alternatively, the contents were removed by nitrogen pressure and transferred into a Schlenk tube for analysis by NMR spectroscopy. The analysis of the reaction solutions by GC, GC–MS or NMR spectroscopy was carried out within 6 h after cooling the autoclave.

Batch autoclave reactions using a methanol–water solvent system. In a batch autoclave reaction carried out using $[RhI_3(CO)(PEt_3)_2]$ as a rhodium source, water (0.9 cm^3, 0.050 mol), methanol (4.1 cm^3, 0.10 mol) and $[RhI_3(CO)(PEt_3)_2]$ (0.015 g, 2.0×10^{-5} mol) were added to an autoclave under a nitrogen atmosphere. After the various components of the reaction solution were added to the autoclave, the procedure was as described above.

Batch autoclave reactions using an ethanoic acid–water solvent system. For autoclave reactions using an ethanoic acid–water solvent system, the reaction solution included $[RhI(CO)(PEt_3)_2]$ (0.022 g, 4.45×10^{-5} mol), methyl ethanoate, (2.2 cm^3, 27 mmol), iodomethane, (0.7 cm^3, 11 mmol), water (1.8 cm^3, 0.10 mol) and ethanoic acid (5.3 cm^3, 0.089 mol). After the various components of the reaction solution were added to the autoclave, the procedure was as described above.

Large scale kinetics rig experiments (300 cm^3 reaction vessel). These experiments were carried out at BP Amoco Chemicals Ltd in Hull in a 300 cm^3 reaction vessel fitted with a bursting disc, catalyst injector, overhead Magnedrive™ stirrer, impeller with gas sparging facility, gas inlet, high pressure (195 bar) carbon monoxide reservoir and thermocouple. Additionally the apparatus featured equipment for pressure measurements and gas sampling. Carbon monoxide consumption was measured by monitoring the pressure drop in the reservoir. A computer collected the data automatically by use of a Dynamic Data Exchange (DDE) link between an Orsi process control package and a data logging package on Excel 7.

For the reactions carried out with an initial water level of 17% w/w, methyl ethanoate (37.67 cm^3, 474 mmol), water (32.80 cm^3, 1.82 mol), iodomethane (24.66 cm^3, 396 mmol) and ethanoic acid (58.04 cm^3, 987 mmol) were added to the autoclave under aerobic conditions. These quantities were altered for reactions incorporating 3% w/w water [methyl ethanoate (22.75 cm^3, 286 mmol), water (6.38 cm^3, 0.35 mol), iodomethane (24.66 cm^3, 396 mmol) and ethanoic acid (102.94 cm^3, 1.75 mol]. The autoclave was sealed, flushed twice with nitrogen and once with carbon monoxide (27 bar), stirring at 500 rpm after each pressurisation and venting the autoclave slowly to ensure the minimum evaporation of the volatile components. The autoclave was then pressurised with carbon monoxide (5 bar) and heated to the required temperature (±0.5 °C) by the use of a heating collar, whilst stirring at 500 rpm.

The catalyst precursor (7.6×10^{-4} mol rhodium), dissolved in ethanoic acid (6.86 cm^3, 117 mmol) and methyl ethanoate (1.07 cm^3, 13.51 mmol) was inserted into the catalyst injector. To initiate the reaction, the catalyst precursor solution was injected into the autoclave. Simultaneously, the autoclave was pressurised with carbon monoxide (27 bar) fed from the high pressure reservoir. On injection of the catalyst solution, the stirring rate was increased to 900 rpm. Data collection was activated prior to the injection of the catalyst solution, but the data used for subsequent calculations was that collected starting 30 s after injection of the catalyst solution. This time was to allow for carbon monoxide to dissolve in the reaction solution. The pressure was maintained at 27 bar by a pressure regulating valve which transferred carbon monoxide from the high pressure reservoir to the reaction vessel as required. The consumption of carbon monoxide from the high pressure reservoir was recorded at 2 s intervals for the duration of the experiment (between 30 and 65 min) and the rate (mol dm^{-3} h^{-1}) was subsequently calculated based on the CO consumption as measured by the pressure drop in the CO reservoir.

After the reaction the autoclave was allowed to cool before a gas sample was collected from the headspace in the autoclave. This gas sample was analysed by gas chromatography using a Chrompack 438S gas chromatograph fitted with a thermal conductivity detector. Gas analysis was carried out for methane, carbon dioxide, carbon monoxide, hydrogen and argon/oxygen. For hydrogen analysis, a molecular sieve (5 Å, 80–100 mesh) column with nitrogen carrier gas was used. For other gases, a Poropak-N and molecular sieve (5 Å, 80–100 mesh) column with hydrogen carrier gas was used.

The autoclave was disconnected from the kinetics rig and a liquid sample of the reaction solution was analysed by gas chromatography using a Chrompack CP900 gas chromatograph fitted with a CP911 autosampler and a flame ionisation detector. A packed column (CB20M) was used with helium as the carrier gas. Liquid analysis was carried out for dimethylether, ethanal, iodoethane, ethyl ethanoate and propanoic acid by-products.

Small scale kinetics rig experiments (30 cm^3 reaction vessel). The apparatus consisted of a reaction vessel (30 cm^3) fitted with a catalyst injection facility, overhead mechanical stirrer, thermocouple, pressure gauge and high pressure carbon monoxide reservoir or 'ballast vessel'. Nitrogen was allowed to pass through the apparatus for 15 min before the reservoir was pressurised with carbon monoxide (*ca.* 90 bar). The reaction solution was previously prepared in a Schlenk tube and typically consisted of methyl ethanoate (1.94 cm^3, 24 mmol), water (2.06 cm^3, 114 mmol), iodomethane (1.55 cm^3, 25 mmol) and ethanoic acid (3.68 cm^3, 63 mmol). The reaction solution was injected into the reaction vessel under anaerobic conditions using a positive pressure of carbon monoxide. The autoclave was pressurised with carbon monoxide (10 bar) and the catalyst precursor, $[RhCl(CO)(PEt_3)_2]$ (0.019 g, 4.81×10^{-5} mol) in a solution of ethanoic acid (0.3 cm^3, 5.10 mmol) and methyl ethanoate (0.2 cm^3, 2.52 mmol) was inserted into the catalyst injection facility. Methyl ethanoate (0.3 cm^3, 3.78 mmol) was also placed in the space above the catalyst injection facility.

The autoclave was heated to 150 °C and the reaction vessel was pressurised with carbon monoxide (22 bar). The system was allowed to stabilise for 5 min and then the catalyst solution was injected with a pressure of carbon monoxide fed from the ballast vessel (27 or 54 bar) to initiate the reaction. Methyl ethanoate (0.3 cm^3, 3.78 mmol) inserted into the space above the catalyst injection facility, washed the walls of the injection facility thus ensuring all of the rhodium complex reached the reaction vessel.

The pressure was maintained at 27 or 54 bar by a pressure regulating valve situated between the reaction vessel and the high pressure reservoir. The carbon monoxide consumption from the high pressure reservoir was recorded manually and the rate (mol dm^{-3} h^{-1}) was calculated.

Reactions studied by NMR spectroscopy

A solution of $[RhI(CO)(PEt_3)_2]$ (0.05–0.1 g, 1.01×10^{-4}–2.02×10^{-4} mol) or $[Rh(OAc)(CO)(PEt_3)_2]$ (0.05 g, 1.17×10^{-4} mol) in CD_2Cl_2 (1 cm^3) was placed in a Schlenk tube. Iodomethane (5.3×10^{-3}–2.5×10^{-2} cm^3, 8.59×10^{-5}–4.04×10^{-4} mol) was added and the solution was analysed by ^{31}P NMR spectroscopy at various time intervals. The solution was warmed slightly or cooled in order to study various reactions.

Variable temperature, high pressure NMR reactions. High pressure NMR studies were carried out in a 5 mm (OD) sapphire tube fitted with a specially designed pressure head.[8]

Solutions of $[RhI(CO)(PEt_3)_2]$ (0.05–0.1 g, 1.01×10^{-4}–2.02×10^{-4} mol) or $[RhMeI_2(CO)(PEt_3)_2]$ (0.07 g, 1.10×10^{-4} mol) in CD_2Cl_2 or C_6D_6 were transferred to the high pressure sapphire NMR tube *via* nitrogen pressure. The NMR tube was sealed and pressurised with carbon monoxide (25–40 bar) in a safety holder. The sapphire tube was carefully placed into the probe of the NMR instrument and the tube was allowed to spin. NMR spectra were recorded at various time intervals or alternatively spectra were recorded at various temperatures of between 100 and −100 °C. For low temperature studies, the sapphire NMR tube was cooled using solid CO_2 until the tube was transferred into the NMR instrument.

Reactions studied by IR spectroscopy

Background spectra, containing all the components of the reaction solution except the catalyst or catalyst precursor were subtracted from the IR spectra of the reaction solutions. Background spectra were recorded at each temperature and pressure used in the reactions.

Kinetic studies

The experiments designed to study the kinetics of various reactions were carried out in a Hastelloy high pressure infrared (HPIR) autoclave produced by Spectratech which operated by circular internal reflectance (CIR) using a silicon CIR rod.[8]

Solutions of $[RhI(CO)(PEt_3)_2]$ or $NBu_4[RhI_2(CO)_2]$, (6.07×10^{-4} mol) in CH_2Cl_2 (9.3 cm^3) were transferred to a deoxygenated high pressure IR autoclave. Iodomethane (0.7 cm^3, 0.011 mol) was added to the injection facility *via* the injection port which was attached to the autoclave. The injection port was sealed and the space above the injection facility was pressurised with nitrogen (5 bar). The IR autoclave was placed in the IR spectrometer. The autoclave was heated to the required temperature using heating rods inserted into the autoclave base. The solution was stirred at 400 rpm *via* an overhead mechanical stirrer. Once the solution temperature was stable, iodomethane (0.7 cm^3, 0.011 mol) was injected from the injection facility into the autoclave body using the pressure of nitrogen. For migratory insertion kinetics studies, $[RhMeI_2(CO)(PEt_3)_2]$ (0.3 g, 4.7×10^{-4} mol) was added to the autoclave as the rhodium source and the autoclave was pressurised with carbon monoxide (27 bar) to initiate the reaction. Simultaneously, on addition of iodomethane or CO, a stop clock was started and IR spectra were recorded every 2 min.

High pressure reactions studied by IR spectroscopy. Solutions of $[RhMeI_2(CO)(PEt_3)_2]$ (0.4 g, 6.29×10^{-4} mol) or $[RhI(CO)(PEt_3)_2]$ (0.3 g, 6.07×10^{-4} mol) in CH_2Cl_2 were transferred to the HPIR autoclave. The autoclave was slowly pressurised with carbon monoxide (1–27 bar) and spectra were recorded to monitor the course of the reaction. Using an alternative solvent system $[RhI(CO)(PEt_3)_2]$ (0.2 g, 4.05×10^{-4} mol) was dissolved in a mixture of ethanoic acid (5.3 cm^3, 89 mmol), methyl ethanoate, (2.2 cm^3, 27 mmol), water (1.8 cm^3, 0.1 mol) and iodomethane (0.7 cm^3, 11 mmol). This solution was added to the HPIR autoclave which was slowly pressurised with carbon monoxide (40 bar). The autoclave was heated to 70 °C and IR spectra were recorded.

Injection of methanol into the high pressure IR autoclave. A solution of $[RhI(CO)(PEt_3)_2]$ (0.25 g, 5.06×10^{-4} mol) in CH_2Cl_2 (9 cm^3) was placed in a Schlenk tube and iodomethane (1 cm^3, 0.016 mol) was added. The solution was transferred to the HPIR autoclave which was pressurised with carbon monoxide (40 bar) for 16 h. Methanol (0.8 cm^3, 0.020 mol) was inserted into the injection facility which was fitted to the autoclave. The space above the injection facility was pressurised with carbon monoxide (65 bar) and the autoclave was heated to 70 °C, while IR spectra were recorded. Methanol (0.8 cm^3, 0.020 mol) was injected into the reaction solution by the pressure of carbon monoxide and IR spectra were recorded to monitor the course of the reaction.

X-Ray crystallography

X-Ray data for $[RhMeI_2(CO)(PEt_3)_2]$ were collected at 220 K on a Rigaku AFC7S diffractometer using graphite-monochromated Mo-Kα radiation ($\lambda = 0.71069$ Å). The structure was solved using direct methods[33] and expanded using Fourier Techniques. The non-hydrogen atoms were refined anisotropically. Hydrogen atoms were included but not refined. Neutral atom scattering factors were taken from the literature.[34] Anomolous dispersion effects were included in F_c. Lorentz polarisation corrections were applied. All calculations were performed using the TEXSAN[35] crystallographic software package. Crystal data, along with the structure solution and refinement parameters are listed in Table 1. CCDC reference number 186/1654. See http://www.rsc.org/suppdata/dt/1999/3771/ for crystallographic files in .cif format.

Table 1 Summary of data collection, structure solution and refinement for $[RhMeI_2(CO)(PEt_3)_2]$

Empirical formula	$RhI_2P_2OC_{14}H_{33}$
Formula weight	636.08
Crystal system	Monoclinic
Space group	*Pn* (no. 7)
Lattice parameters	
a/Å	7.402(5)
b/Å	11.785(5)
c/Å	12.520(4)
β/°	96.01(4)
V/Å^3	1086.2(9)
Z	2
μ(Mo-Kα)/cm^{-1}	37.71
T/K	220.0
No. observations [$I > 3.00\sigma(I)$]	2453
No. variables	178
Reflection/parameter ratio	13.78
Residuals: R, R_w	0.026, 0.027
Goodness of fit indicator	4.04

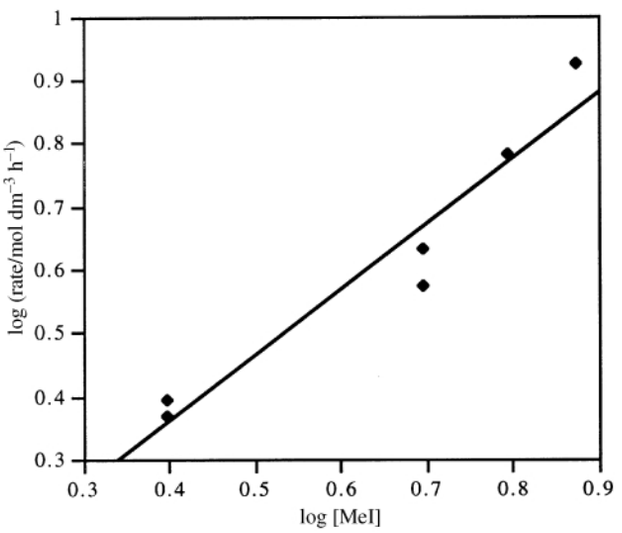

Fig. 1 Dependence of the rate of carbonylation of methanol upon [MeI] using $[RhCl(CO)(PEt_3)_2]$ as catalyst precursor.

Results and discussion

Catalytic reactions

Initial reaction rates. The carbonylation of methanol using $[RhX(CO)(PEt_3)_2]$ (X = OAc, Cl or I) or $[RhCl(CO_2)]_2$ as catalyst precursors was carried out in a reactor attached to a ballast vessel in such a way that the pressure in the reactor was maintained constant and the drop of pressure in the ballast vessel was used to monitor the kinetics of the reaction. Initial rates at 150 and 120 °C are shown in Table 2 for reactions carried out in the presence of an initial water concentration of 17%. These show that $[RhCl(CO)(PEt_3)_2]$ is a significantly more active catalyst for methanol carbonylation than $[RhCl(CO)_2]_2$. Both the temperatures used are lower than the normal operating temperature (160–200 °C) for $[Rh(CO)_2I_2]^-$, which is formed *in situ* from $[RhCl(CO)_2]_2$, but studies at higher temperatures showed that the lifetime of $[RhX(CO)(PEt_3)_2]$ was very short. Fig. 1 presents the dependence of the initial rate of methanol carbonylation on [MeI], showing that the reaction is first order in [MeI] at 150 °C. A reaction carried out at $p_{CO} = 54$ bar had the same rate as one carried out at $p_{CO} = 27$ bar (Table 2). Although there are only two data points, they suggest a zero order dependence on p_{CO} at least between 27 and 54 bar. These dependencies suggest that, as with $[RhI_2(CO)_2]^-$,[1,3,4] the rate determining step in the carbonylation of methanol is oxidative addition of MeI to the Rh^I centre.

Water is essential for the activity and stability of rhodium

Table 2 Kinetic data for the carbonylation of methanol[a]

Catalyst precursor	T/°C	p_{CO}/bar	Initial [water] (%)(w/w)	Initial rate/ mol dm^{-3} h^{-1}	Steady state rate/ mol dm^{-3} h^{-1}	TOF[b]/h^{-1}
[RhCl(CO)(PEt$_3$)$_2$]	150	27	17.1	9.2	5.0	1573
[RhCl(CO)$_2$]$_2$	150	27	17.1	5.0	5.0	1052
[RhCl(CO)(PEt$_3$)$_2$]	120	27	17.1	1.6	1.2	336
[RhCl(CO)$_2$]$_2$	120	27	17.1	0.9	1.2	252[c]
[RhCl(CO)(PEt$_3$)$_2$]	120	27	3.3	0.6		126
[RhCl(CO)$_2$]$_2$	120	27	3.3	0.6		126
[RhCl(CO)(PEt$_3$)$_2$]	150	27	17.1	2.5[d]		526
[RhCl(CO)(PEt$_3$)$_2$]	150	54	17.1	2.5[d]		526

[a] Conditions as for large-scale kinetics rig (see Experimental section). [b] Initial turnover frequency, mol of CO consumed (mol Rh)$^{-1}$ h^{-1}. [c] TOF at steady state. [d] Conditions as for small-scale kinetics rig (see Experimental section).

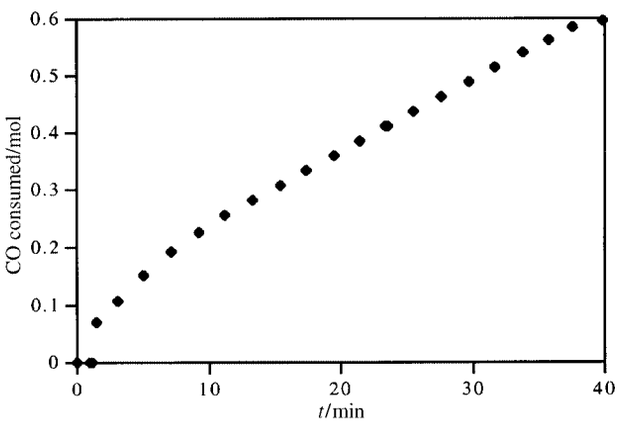

Fig. 2 Uptake of CO during the carbonylation of methanol at 150 °C using [RhCl(CO)(PEt$_3$)$_2$] as catalyst precursor.

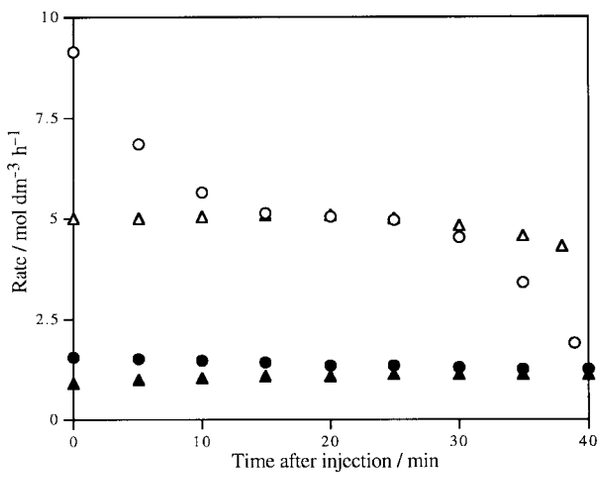

Fig. 3 Time dependence of the rate of carbonylation of methanol using [RhCl(CO)(PEt$_3$)$_2$] (○, 150 °C; ●, 120 °C) or [RhCl(CO)$_2$]$_2$ (△, 150 °C; ▲, 120 °C) as catalyst precursors.

based methanol carbonylation catalysts, but increases the cost and complexity of the product recovery process. We have, therefore, investigated the reactivity of the [RhCl(CO)(PEt$_3$)$_2$] system at low water (3% w/w) concentration. The initial rate of this reaction at 120 °C was 0.6 mol dm^{-3} h^{-1}, the same as that observed using [RhCl(CO)$_2$]$_2$ so no enhancement is observed using the more electron rich metal centre under these low water conditions, [RhCl(CO)(PEt$_3$)$_2$] is inactive for the carbonylation of methyl ethanoate to ethanoic anhydride under anhydrous conditions. Similarly, very low activity was observed using HCl or HBr in place of HI or MeI in these reactions.

Catalyst stability. A kinetic profile for the carbonylation of methanol at 150 °C in the presence of water (17% w/w) and [RhCl(CO)(PEt$_3$)$_2$] is shown in Fig. 2 and the first derivative of this plot (*i.e.* the variation of the reaction rate with time) is shown in Fig. 3. Three different regions are apparent. The high initial rate falls off over the first 15 min before levelling off at a rate of 5 mol dm^{-3} h^{-1} for 15 min and then falling again. The reaction was terminated after 40 min. Also shown in Fig. 3 is the rate profile using [RhCl(CO)$_2$]$_2$ as catalyst precursor, which is stable at 5 mol dm^{-3} h^{-1} throughout the reaction with only a small decrease in rate at the end of the reaction. The fact that both catalyst precursors give identical steady-state rates during the middle parts of the reaction suggest that the active species during this period is the same and this is confirmed by IR studies which show that the species present at the end of the reaction starting with [RhCl(CO)(PEt$_3$)$_2$] is *trans*-[RhI$_4$(CO)$_2$]$^-$ (ν_{CO} = 2090 cm^{-1}).

The rate profiles for [RhCl(CO)(PEt$_3$)$_2$] and [RhCl(CO)$_2$]$_2$ as precursors at 120 °C are also shown in Fig. 3. These again show that [RhCl(CO)(PEt$_3$)$_2$] degrades to [Rh(CO)$_2$I$_2$]$^-$, although its lifetime is extended at this lower temperature. The initial rise in activity of the system containing [RhCl(CO)$_2$]$_2$ presumably indicates that the active species, [RhI$_2$(CO)$_2$]$^-$ is not formed instantaneously under these low temperature conditions.

The fall off in rate after 30 min for the reaction carried out at 150 °C in the presence of [RhCl(CO)(PEt$_3$)$_2$] can partly be attributed to the lower methanol concentration as the reaction nears completion. All of the substrate methyl ethanoate (0.488 mol) is consumed after *ca.* 30 min and thereafter the MeI is reacting. In addition, however, under the conditions used in this study [eqn. (1)] water is consumed during the reaction

$$\mathrm{MeOAc + CO + H_2O \longrightarrow 2HOAc} \qquad (1)$$

and hence at the end of the reactions the water concentration is low.

This results in an increase in the amount of [Rh(CO)$_2$I$_4$]$^-$, since one of the rôles of water is to reduce [Rh(CO)$_2$I$_4$]$^-$ back to the active [Rh(CO)$_2$I$_2$]$^-$.[2] Water also hydrates HI, thus reducing its ability to oxidatively add to [Rh(CO)$_2$I$_2$]$^-$ and start the process for the formation of [Rh(CO)$_2$I$_4$]$^-$ shown in Scheme 1. The drop in methyl ethanoate concentration in the reaction solution will also lead to an increase in [HI] since this is kept low by eqn. (2) when methyl ethanoate is in excess.

$$\mathrm{MeOAc + HI \rightleftharpoons MeI + HOAc} \qquad (2)$$

The reactions that lead to the formation of [RhI$_4$(CO)$_4$]$^-$ and to its recycling to [RhI$_2$(CO)$_2$]$^-$ are shown in Scheme 1.

Less drop in rate is observed at the end of the reaction catalysed by [RhCl(CO)$_2$]$_2$ because the absence of the fast initial stage of the reaction means that the conversion after any given time is lower than for [RhCl(CO)(PEt$_3$)$_2$] and the concentration of [RhI$_4$(CO)$_2$]$^-$ will rise later.

Product analysis

As expected, because the active species is essentially the same

Table 3 Side product analysis for the carbonylation of methanol with different catalyst precursors[a]

By-product	Catalyst	
	$[RhCl(CO)(PEt_3)_2]$	$[RhCl(CO)_2]_2$
Hydrogen	3.8	1.9
Carbon dioxide	0.6	0.3
Methane	<0.1[b]	<0.1[b]
Ar/O_2	0.7	0.14
Dimethyl ether	1.33	1.30
Ethanal	1.48	1.39
Iodoethane	0.416	0.199
Ethyl ethanoate	0.295	0.239
Propanoic acid	0.986	0.824

[a] Conditions as for large-scale kinetics rig (see Experimental section), 150 °C, $p_{CO} = 27$ bar, 40 min. Gases as % (v/v), dissolved liquids as concentration/10^{-3} mol dm^{-3}. [b] Detection limit = 0.1%.

Table 4 ^{31}P NMR spectral data for rhodium complexes in CD_2Cl_2 at −20 °C

Complex	δ	J_{RhP}/Hz
$[Rh(OAc)(CO)(PEt_3)_2]$	24.6	123.5
$[RhI(CO)(PEt_3)_2]$	20.2	111.2
$[RhMe(OAc)I(CO)(PEt_3)_2]$	21.3	85.4
$[RhMeI_2(CO)(PEt_3)_2]$	2.4	85.5
$[Rh(COMe)I_2(CO)(PEt_3)_2]$[a]	2.1	88.2
$[RhI(CO)_2(PEt_3)_2]$[b]	30.5	84.1
$[RhI_3(CO)(PEt_3)_2]$[a]	−4.4	74.1
$[RhHI_2(CO)(PEt_3)_2]$[a]	12.9	80.0

[a] 25 °C. [b] −40 °C.

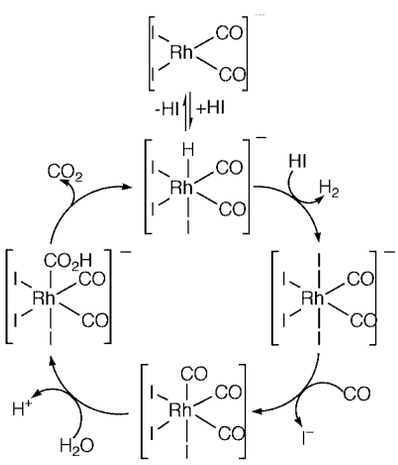

Scheme 1 Water gas shift chemistry occurring during the carbonylation of methanol catalysed by $[RhI_2(CO)_2]^-$.[1]

for reactions involving $[RhCl(CO)(PEt_3)_2]$ or $[RhCl(CO)_2]_2$ as catalyst precursor, the reaction side product distribution is similar (see Table 3) for both catalysts at 150 °C with only the water–gas shift products, H_2 and CO_2 being significantly higher for $[RhCl(CO)(PEt_3)_2]$ because of the higher extent of reaction. The homologation products, iodoethane and ethyl ethanoate are also somewhat increased but still remain very low.

Active species

The reaction of iodomethane (2 equivalents) with $[Rh(OAc)(CO)(PEt_3)_2]$[7] was monitored by ^{31}P NMR spectroscopy (NMR data for the complexes are collected in Table 4 and the Experimental section). The reagents were mixed at −20 °C and the reaction monitored on warming to 30 °C. At −20 °C, three doublets assigned to $[Rh(OAc)(CO)(PEt_3)_2]$,[7] $[RhI(CO)(PEt_3)_2]$[10] and the rhodium(III) complex, $[RhMeI(OAc)(CO)(PEt_3)_2]$ were detected. On warming, the relative intensities of these species changed and a new doublet from $[RhMeI_2(CO)(PEt_3)_2]$ appeared. At 30 °C, $[RhI(CO)(PEt_3)_2]$ and $[RhMeI_2(CO)(PEt_3)_2]$ but not the acetate complexes were dominant. MeOAc was also observed by GC–MS. These reactions confirm that $[RhI(CO)(PEt_3)_2]$ is the active catalytic species and this was used for all subsequent mechanistic studies. It is assumed that this is also the active species if $[RhCl(CO)(PEt_3)_2]$ is the catalyst precursor.

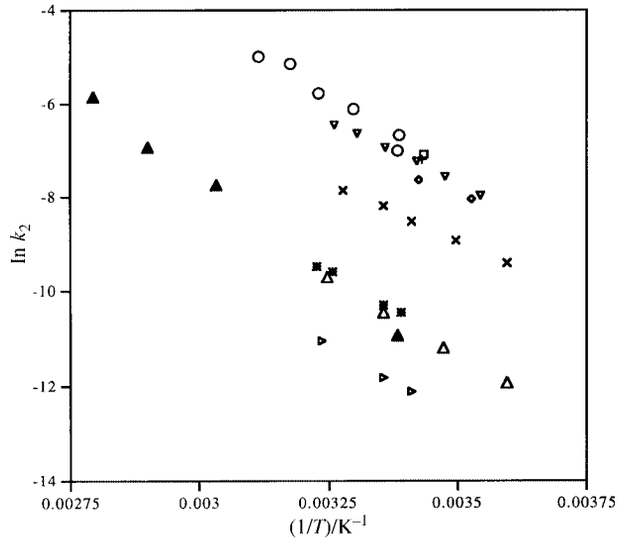

Fig. 4 Arrhenius plots for the oxidative addition of MeI to $[RhI_2(CO)_2]^-$ (△, literature data,[42] ▲, this work) or $[RhX(CO)L_2]$. ○, L = PEt_3, X = I; +, L = PBu_3, X = Cl;[37] □, L = $P(C_8H_{17})_3$, X = Cl;[37] ◇, L = $P(C_{18}H_{37})_3$, X = Cl;[37] *, L = PPh_3, X = Cl;[36] ×, L = $P(C_6H_4OMe\text{-}4)_3$, X = Cl;[36] ▷, L = $P(C_6H_4F\text{-}4)_3$, X = Cl;[36] ▽, L_2= $Ph_2PCH_2P(S)Ph_2$, X = I.[51]

Oxidative addition of MeI

Oxidative addition of MeI to complexes of the form $[RhX(CO)(PR_3)_2]$ has been extensively studied[36–40] and can lead to $[RhMeXI(CO)(PR_3)_2]$ (R = alkyl)[37,38] or to $[Rh(COMe)IX(PR_3)_2]$, (R = aryl).[36,39,40] Kinetic studies show that the rate of oxidation addition is higher for trialkyl phosphines,[37,38] as expected because of the more electron rich metal centre, but decreases for very long chain alkyls, probably for steric reasons. Plots of log k *vs.* $1/T$ for various phosphines are shown in Fig. 4. An S_N2 mechanism has been proposed for the oxidative addition with the added halide ending up *trans* to the methyl group. We have also shown this to be the case for CH_2I_2[41] and for allylic halides.[8]

^{31}P and ^1H NMR studies confirmed that $[RhI(CO)(PEt_3)_2]$ reacts with MeI to give a rhodium(III) species, which we have fully characterised as $[RhMeI_2(CO)(PEt_3)_2]$. The X-ray structure of this complex is shown in Fig. 5 and confirms that the complex has *trans* phosphines and that the methyl group is *trans* to I. In order to investigate the relative reactivities of $[RhI(CO)(PEt_3)_2]$ and $[Rh(CO)_2I_2]^-$, we measured the rate of the reaction of the rhodium complex with iodomethane in a high-pressure IR cell at a variety of temperatures. Iodomethane was injected into the reactor once the temperature had stabilised and the IR spectrum was recorded after various times. A typical decay profile is shown in Fig. 6 and the linearity of the log plot in Fig. 7. The Arrhenius plots for $[RhI(CO)(PEt_3)_2]$ and for $[RhI_2(CO)_2]^-$ (both measured by us using the decay of the peak at 1988 cm^{-1} and from the literature[42]) are included in Fig. 4 and it is apparent that the rate is higher for $[RhI(CO)(PEt_3)_2]$ at all the temperatures studied than for any other complexes of the form $[RhX(CO)(PR_3)_2]$ and at 298 K is 57 times higher than for $[RhI_2(CO)_2]^-$, confirming that the increased electron density on the rhodium complex leads to a higher

Table 5 Activation enthalpy ($\Delta H^{\ddagger}$), entropy ($\Delta S^{\ddagger}$) and Gibbs free energy ($\Delta G^{\ddagger}$) and rate at 298 K for the oxidative addition of iodomethane to $[RhI(CO)(PEt_3)_2]$ and $[RhI_2(CO)_2]^-$

Complex	Solvent	$\Delta H^{\ddagger}_{298}$/ kJ mol^{-1}	$\Delta S^{\ddagger}_{298}$/ J mol^{-1} K^{-1}	$\Delta G^{\ddagger}_{298}$/ kJ mol^{-1}	Rate[a]/ mol dm^{-3} s^{-1}
$[RhI(CO)(PEt_3)_2]$	CH_2Cl_2	56 ± 13	−112 ± 44	89 ± 26	7.8×10^{-5}
$[RhI_2(CO)_2]^-$	CH_2Cl_2	68 ± 8	−105 ± 22	99 ± 15	
$[RhI_2(CO)_2]^-$ [b]	MeI	50 ± 1	−165 ± 4	99 ± 1	

[a] [Rh] = 0.06 mol dm^{-3}. [b] From ref. 42.

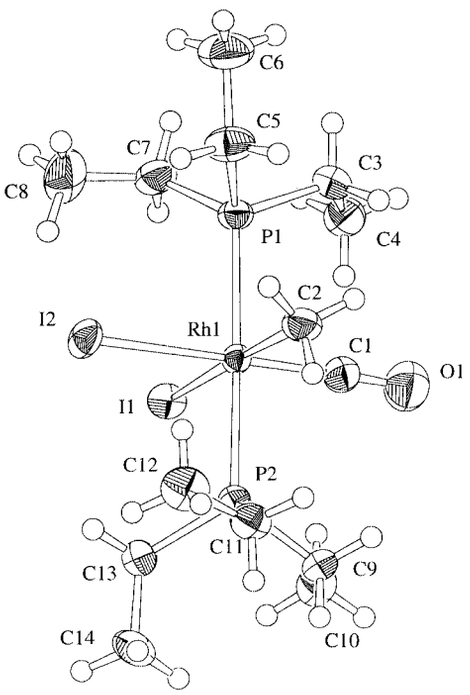

Fig. 5 X-Ray structure and numbering scheme for $[RhMeI_2(CO)(PEt_3)_2]$.

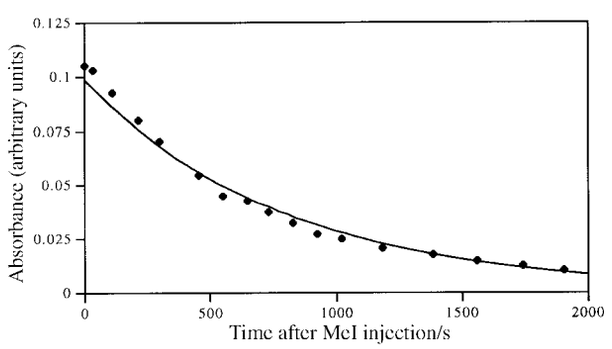

Fig. 6 Plot of IR absorbance intensity at 1961 cm^{-1} (ν_{CO} for $[RhI(CO)(PEt_3)_2]$) *vs.* time during the reaction of $[RhI(CO)(PEt_3)_2]$ with MeI at 22 °C in CH_2Cl_2.

rate of oxidative addition. The activation parameters for $[RhI(CO)(PEt_3)_2]$ and for $[RhI_2(CO)_2]^-$, as determined by us and as reported in the literature[42] are collected in Table 5 and show that the main difference appears to be in the enthalpy of activation. The large increase in rate of oxidation addition of MeI to $[RhI(CO)(PEt_3)_2]$ compared with $[Rh(CO)_2I_2]^-$ is not reproduced in the rate of the overall catalytic reaction (1.8 times faster at 150 °C). This presumably reflects slightly different activation energies for the two oxidative addition reactions, but the scatter on the data does not allow us to extrapolate to the much higher temperature. We note also that the rates of the oxidative addition reactions were measured in CH_2Cl_2, a much less polar medium than that in which the catalytic experiments were carried out.

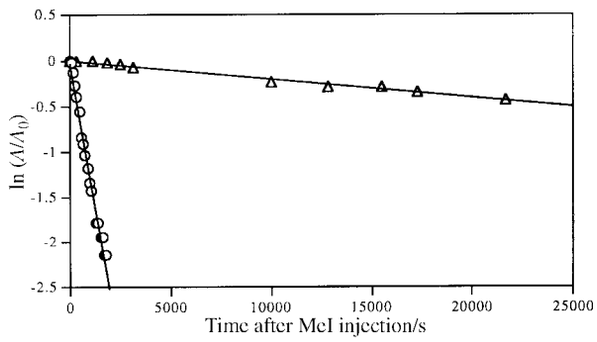

Fig. 7 Dependence of the intensity of ν_{CO} of the rhodium starting materials with time during the oxidative addition of MeI to $[RhI(CO)(PEt_3)_2]$ (○) or $[RhI_2(CO)_2]^-$ (△) at 22 °C in CH_2Cl_2.

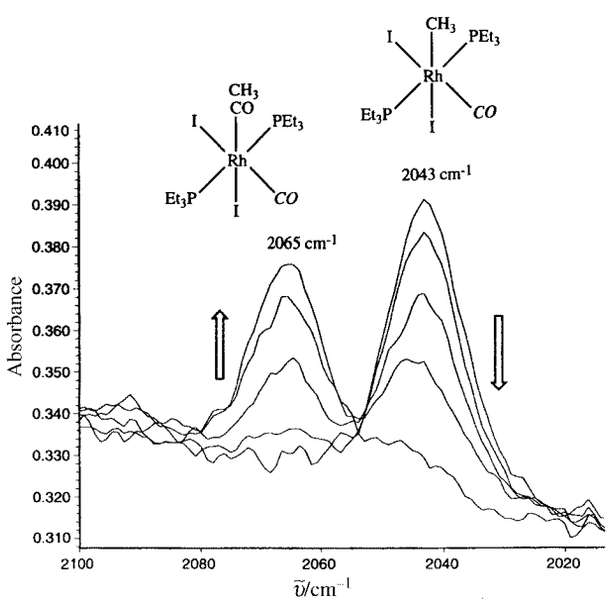

Fig. 8 Changes in the IR spectrum during the reaction of CO (27 bar) with $[RhMeI_2(CO)(PEt_3)_2]$ at 23 °C in CH_2Cl_2.

Formation of the acyl intermediate

Because $[RhMeI_2(CO)(PEt_3)_2]$ is stable, it is straightforward to measure the rate of formation of $[Rh(COMe)I_2(CO)(PEt_3)_2]$ from reaction with CO. $[RhMeI_2(CO)(PEt_3)_2]$ in CH_2Cl_2 was placed in the HPIR cell and heated to the desired temperature. CO was then introduced and the IR spectrum monitored with time. The bands from $[RhMeI_2(CO)(PEt_3)_2]$ decreased with time, whilst new bands grew in at 2065 (ν_{CO}) and 1665 ($\nu_{C=O}$). Fig. 8 shows a typical plot showing the decrease of the band at 2043 cm^{-1} (ν_{CO} for $[RhMeI_2(CO)(PEt_3)_2]$) and an increase of the band at 2065 cm^{-1} (ν_{CO} for $[Rh(COMe)I_2(CO)(PEt_3)_2]$). The measurement of the rate of insertion was carried out at 22.8 °C at both 27 bar ($k_{obs} = 7.1 \times 10^{-5}$ mol dm^{-3} s^{-1}) and 40 bar ($k_{obs} = 1.1 \times 10^{-4}$ mol dm^{-3} s^{-1}) tentatively suggesting that the insertion reaction is first order in p_{CO}, *i.e.* $k_{-1} \ll k_2$[CO] (Scheme 2). This contrasts with the situation for $[RhMeI_3(CO)_2]^-$, for which the rate of the insertion reaction is

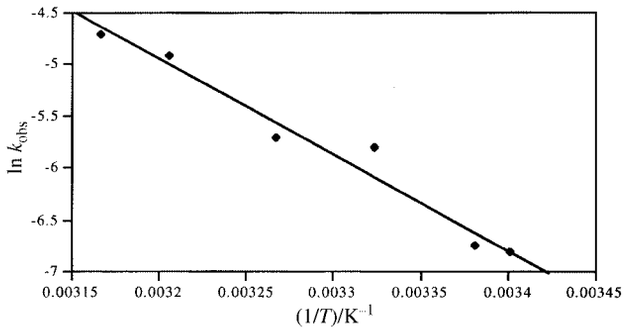

Fig. 9 Temperature dependence for the reaction of CO (27 bar) with $[RhMeI_2(CO)(PEt_3)_2]$ in CH_2Cl_2.

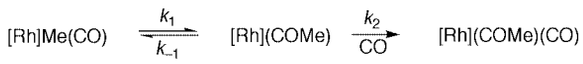

Scheme 2 Mechanism of insertion of CO into the Rh–Me bond.

independent of p_{CO} and $k_2[CO] \gg k_{-1}$.[42] This difference in the dependence of the rate of formation of the acyl complexes on p_{CO} between $[RhMeI_2(CO)(PEt_3)_2]$ and $[RhI_2(CO)_2]^-$ indicates a difference in the thermodynamic stabilities for the various intermediates. For the PEt_3 complex, the five coordinate insertion product, $[Rh(COMe)I_2(PEt_3)_2]$, is thermodynamically at higher energy than the starting $[RhMeI_2(CO)(PEt_3)_2]$ and the insertion reaction is only driven when the five-coordinate intermediate is trapped by CO; whilst for $[RhMeI_3(CO)_2]^-$, the insertion reaction occurs spontaneously even in the absence of CO and the five-coordinate intermediate is thermodynamically favoured.[4]

The temperature dependence of the formation of the acyl complex is shown in Fig. 9 but it is not possible to calculate meaningful activation parameters for this reaction since k_{obs} is a composite of k_1, k_{-1} and k_2, each of which may have quite different temperature dependencies. The values of k_{obs} for the formation of $[Rh(COMe)I_2(CO)(PEt_3)_2]$ and of $[Rh(COMe)I_3(CO)_2]^-$ from $[RhMeI_2(CO)(PEt_3)_2]$ and $[RhMeI_3(CO)_2]^-$ were compared at 23 °C and 27 bar. This showed that, under these conditions, this step is 38 times faster for $[RhMeI_2(CO)_3]^-$.

Despite the increase in rate of the oxidative addition reaction by 57 times and the decrease in rate of formation of the acyl complex for $[RhMeI_2(CO)(PEt_3)_2]$ compared with $[RhMeI_3(CO)_2]^-$, the oxidative addition step still remains rate determining in the overall catalytic carbonylation of methanol. The absolute rates of the oxidative addition reaction (7.8×10^{-5} mol dm^{-3} s^{-1}) and CO insertion (7.1×10^{-5} mol dm^{-3} s^{-1}) under identical conditions at 298 K are very similar (Table 5). It should be remembered, however, that the rates of the individual steps were measured near room temperature, far away from the temperature at which the catalytic reaction rates were measured (120 and 150 °C) and in a medium of very different polarity. There is also some evidence (see later) that, in the absence of water, reductive elimination of MeCOI may be rate determining. Attempts were made to isolate $[Rh(COMe)I_2(CO)(PEt_3)_2]$ by the reaction of $[RhMeI_2(CO)(PEt_3)_2]$ with CO under pressure or by reaction of $[RhI(CO)(PEt_3)_2]$ with MeCOCl followed by exchange of Cl^- with I^-. Although both produced the desired product, attempting to isolate it in the absence of an excess of CO led to loss of CO and the product was always contaminated with $[RhMeI_2(CO)(PEt_3)_2]$.

Reductive elimination of MeCOI

In the carbonylation of methanol catalysed by $[RhI_2(CO)_2]^-$ it is generally considered that the product is released from the metal by reductive elimination of MeCOI from $[Rh(COMe)I_3(CO)_2]^-$ for subsequent hydrolysis to ethanoic acid.[1]

Since reductive elimination involves reduction of Rh^{III} to Rh^{I}, it is possible that increasing the electron density on the metal, *e.g.* by adding trialkylphosphines, may disfavour this step and even make it rate determining. We, therefore, investigated the reductive elimination reaction.

$[RhI(CO)(PEt_3)_2]$ was first reacted with an excess of MeI in the HPIR cell at 25 °C. The cell was pressurised with CO (40 bar) for 16 h to generate $[Rh(COMe)I_2(CO)(PEt_3)_2]$. The autoclave was then heated to 70 °C and an absorption appeared at 1798 cm^{-1}, consistent with the formation of ethanoyl iodide.[43] To confirm that MeCOI had formed, methanol was injected into the cell and the peak at 1798 cm^{-1} was replaced by one at 1745 cm^{-1} (methyl ethanoate). The formation of methyl ethanoate was further confirmed by GCMS analysis of the solution after depressurisation. The reactions occurring are shown in Scheme 3.

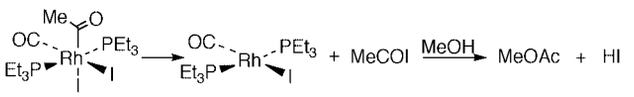

Scheme 3 Reductive elimination of MeCOI from $[Rh(MeCO)I_2(CO)(PEt_3)_2]$ and subsequent formation of MeOAc.

All of the steps in the catalytic carbonylation reaction have been demonstrated separately, as shown in Scheme 4.

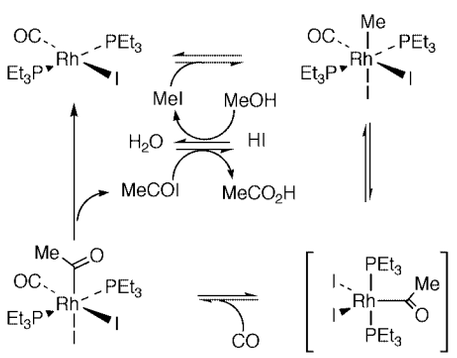

Scheme 4 Full catalytic cycle for the carbonylation of methanol catalysed by $[RhI(CO)(PEt_3)_2]$. The compound in square brackets has not been observed.

Reaction of $[RhI(CO)(PEt_3)_2]$ with CO

During the course of studies of the oxidative addition of MeI to $[RhI(CO)(PEt_3)_2]$ and the subsequent insertion of CO into the Rh–Me bond, it became apparent that a reaction might be occurring between $[RhI(CO)(PEt_3)_2]$ and CO. We, therefore, studied this reaction by HPIR and HP NMR spectroscopy (Fig. 10). At 25 °C the doublet from $[RhI(CO)(PEt_3)_2]$ in the ^{31}P NMR spectrum (δ 20.2, $J_{RhP} = 112$ Hz) is replaced by a broad doublet (δ 28.1, $J_{RhP} = 90$ Hz) when treated with CO (25 bar). On cooling, this doublet broadens further before sharpening at −40 °C to one doublet (no resolution into more than one doublet) at (δ 30.5, $J_{RhP} = 84$ Hz), which was unchanged down to −70 °C. In the ^{13}C NMR spectra, a broad singlet from the C atom of CO at δ 192.7 sharpened on cooling to a doublet of triplets (δ 192.5, $J_{RhC} = 71.7$, $J_{PC} = 14.9$ Hz). Similar changes were observed in the low-temperature NMR spectra of $[RhCl(CO)(PEt_3)_2]$ under CO, except that two different species were observed at low temperature.[8] Studying the same reaction by HPIR spectroscopy the absorption from ν_{CO} in $[RhI(CO)(PEt_3)_2]$ was replaced by new absorptions at 1943s and 1999w cm^{-1}.

These changes in the NMR and IR spectra are reversible on removing the CO pressure, so it is not possible to isolate the complex formed. However, the spectroscopic properties are consistent with the reaction between $[RhI(CO)(PEt_3)_2]$ and CO

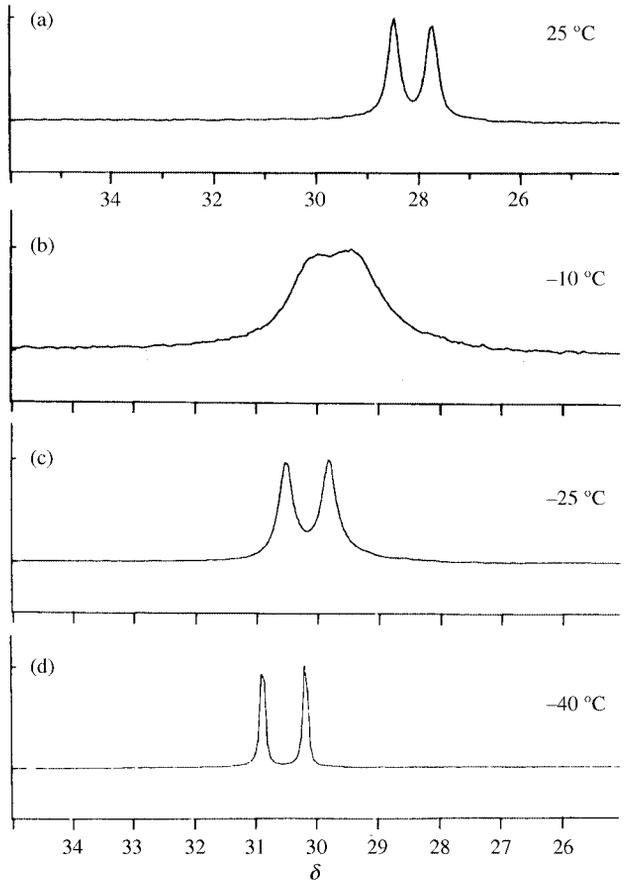

Fig. 10 ^{31}P NMR spectra for a solution containing [RhI(CO)(PEt$_3$)$_2$] under CO (25 bar). (a) 25 °C; (b) −10 °C; (c) −25 °C; (d) −40 °C.

leading to [RhI(CO)$_2$(PEt$_3$)$_2$] [eqn. (3)] and to an equilibrium

$$[RhI(CO)(PEt_3)_2] + CO \rightleftharpoons [RhI(CO)_2(PEt_3)_2] \quad (3)$$

being set up between the mono- and di-carbonyls which occurs on a timescale similar to that of the NMR experiment. On warming, the equilibrium lies to the side of the monocarbonyl, although complete formation of the dicarbonyl occurs at −40 °C. The four possible structures for the dicarbonyl which have equivalent PEt_3 groups and equivalent CO ligands (as required by the ^{31}P and ^{13}C NMR spectra) are shown in Fig. 11. The relative intensities of the IR bands suggest that the two CO ligands are not mutually *trans* but that the angle is large so that [RhI(CO)$_2$(PEt$_3$)$_2$] has structure **b** or **d** (Fig. 11). The isomer of [RhCl(CO)$_2$(PEt$_3$)$_2$] stable at higher temperatures was also assigned a structure analogous to **b** or **d**.

Under catalytic conditions, eqn. (3) will be of little importance since at 120 °C the reaction lies totally to [RhI(CO)(PEt$_3$)$_2$]. Furthermore, addition of MeI to a solution of [RhI(CO)(PEt$_3$)$_2$] under CO (40 bar) produced [RhMeI$_2$(CO)(PEt$_3$)$_2$], as indicated by IR and NMR spectroscopies. Signals from [RhI(CO)$_2$(PEt$_3$)$_2$] were not observed.

Catalyst deactivation

The kinetic results presented above suggest that the initial catalytically active species, [RhI(CO)(PEt$_3$)$_2$] decomposes over time to give [RhI$_2$(CO)$_2$]$^-$. In order to study this deactivation in more detail, we carried out catalytic reactions using methanol containing MeI as substrate in batch autoclaves, stopping the reactions after 1 h at a given temperature. The autoclaves were cooled, vented and the ^{31}P NMR spectra of the liquids recorded at ambient temperature under argon. The results with the assignments of the peaks are shown in Fig. 12(a)–(c). After heating at 80 °C and cooling to ambient temperature, the major

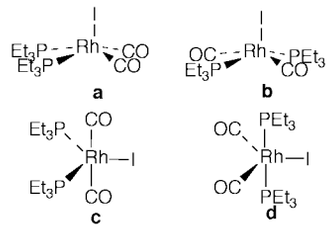

Fig. 11 Possible structures for [RhI(CO)$_2$(PEt$_3$)$_2$].

species present are [RhMeI$_2$(CO)(PEt$_3$)$_2$] and [Rh(COMe)I$_2$(CO)(PEt$_3$)$_2$] together with a doublet at δ 12.9 (J_{PRh} = 80 Hz) assigned to [RhHI$_2$(CO)(PEt$_3$)$_2$] by comparison with a sample prepared from the reaction of [RhI(CO)(PEt$_3$)$_2$] with aqueous HI. In addition, small amounts of [RhI(CO)(PEt$_3$)$_2$] in slow exchange with [RhI(CO)$_2$(PEt$_3$)$_2$], [Et$_3$PMe]I, Et$_3$PO and doublets at δ 32 (J_{PRh} = 124.4 Hz) and δ −4.4 (J_{PRh} = 74.1 Hz) were observed. The resonance at δ −4.4 is assigned to [RhI$_3$(CO)(PEt$_3$)$_2$][7] by comparison with an authentic sample prepared from [RhI(CO)(PEt$_3$)$_2$] and I$_2$, whilst that at δ 32 is unassigned but may arise from a monophosphine complex.

After 1 h at 100 °C followed by cooling to ambient temperature, the major species are [RhMeI$_2$(CO)(PEt$_3$)$_2$] and [Rh(COMe)I$_2$(CO)(PEt$_3$)$_2$]; the signal from [RhHI$_2$(CO)(PEt$_3$)$_2$] has decreased significantly in intensity and those from Et$_3$PO and the supposed monophosphine species have become more important. After heating at 120 °C and cooling, the major species is [RhI$_3$(CO)(PEt$_3$)$_2$] whilst the signals from the supposed monophosphine complexes and especially Et$_3$PO have increased markedly. A ^{13}C NMR spectrum of this solution showed, in addition to the triplets expected from the P*C*H$_2$CH$_3$ of *trans* bis-PEt$_3$ species, a doublet at δ 23.4 (J_{RhC} = 32.3 Hz) from a monophosphine species. At 140 °C, total loss of Et$_3$P from the rhodium occurred (no P–Rh coupled signals) to give mainly Et$_3$PO and a small amount of Et$_3$PMeI.

Since oxidative addition of iodomethane is believed to be rate determining in the carbonylation of methanol catalysed by [RhI(CO)(PEt$_3$)$_2$], it is not expected that [Rh(COMe)I$_2$(CO)(PEt$_3$)$_2$] and its decarbonylation product should be the dominant species, but rather [RhI(CO)(PEt$_3$)$_2$]. The observation that the methyl and ethanoyl complexes dominate the spectrum under low temperature conditions suggests that, in the absence of water, reductive elimination of ethanoyl iodide may be rate determining. [RhHI$_2$(CO)(PEt$_3$)$_2$] is also unexpected but probably arises from the oxidative addition of HI, produced from eqn. (4), with [RhI(CO)(PEt$_3$)$_2$], which is also observable in the solution from the reaction carried out at 80 °C.

$$MeCOI + MeOH \longrightarrow MeCOOMe + HI \quad (4)$$

If the reaction is carried out using MeOD, only MeCO$_2$Me is produced confirming that [RhHI$_2$(CO)(PEt$_3$)$_2$] is not formed by β-H abstraction in [Rh(MeCO)(CO)$_x$I$_2$(PEt$_3$)$_2$] (x = 0 or 1), which would give CH$_2$DCO$_2$Me *via* ketene.[7]

At higher temperatures, [RhHI$_2$(CO)(PEt$_3$)$_2$] is much less important. In order to try to understand this, we stirred [RhHI$_2$(CO)(PEt$_3$)$_2$] in methanol for 16 h. The products were [RhI(CO)(PEt$_3$)$_2$] (70%), [RhI$_3$(CO)(PEt$_3$)$_2$] (21%) and unreacted [RhHI$_2$(CO)(PEt$_3$)$_2$] (9%). Clearly, the oxidative addition of HI to [RhI(CO)(PEt$_3$)$_2$] is reversible, with the HI presumably reacting with methanol to regenerate MeI and the positive $\Delta S^{\ominus}$ of the reductive elimination ensuring that [RhHI$_2$(CO)(PEt$_3$)$_2$] is not favoured at higher temperature. This experiment also suggests, however, that [RhI$_3$(CO)(PEt$_3$)$_2$] can be generated from [RhHI$_2$(CO)(PEt$_3$)$_2$], presumably *via* protonation by HI, in a sequence of reactions analogous to those involved in the production of [RhI$_4$(CO)$_2$]$^-$ from [RhI$_2$(CO)$_2$]$^-$ in the Monsanto system.[1]

The higher temperature reactions suggest that [RhI$_3$(CO)-

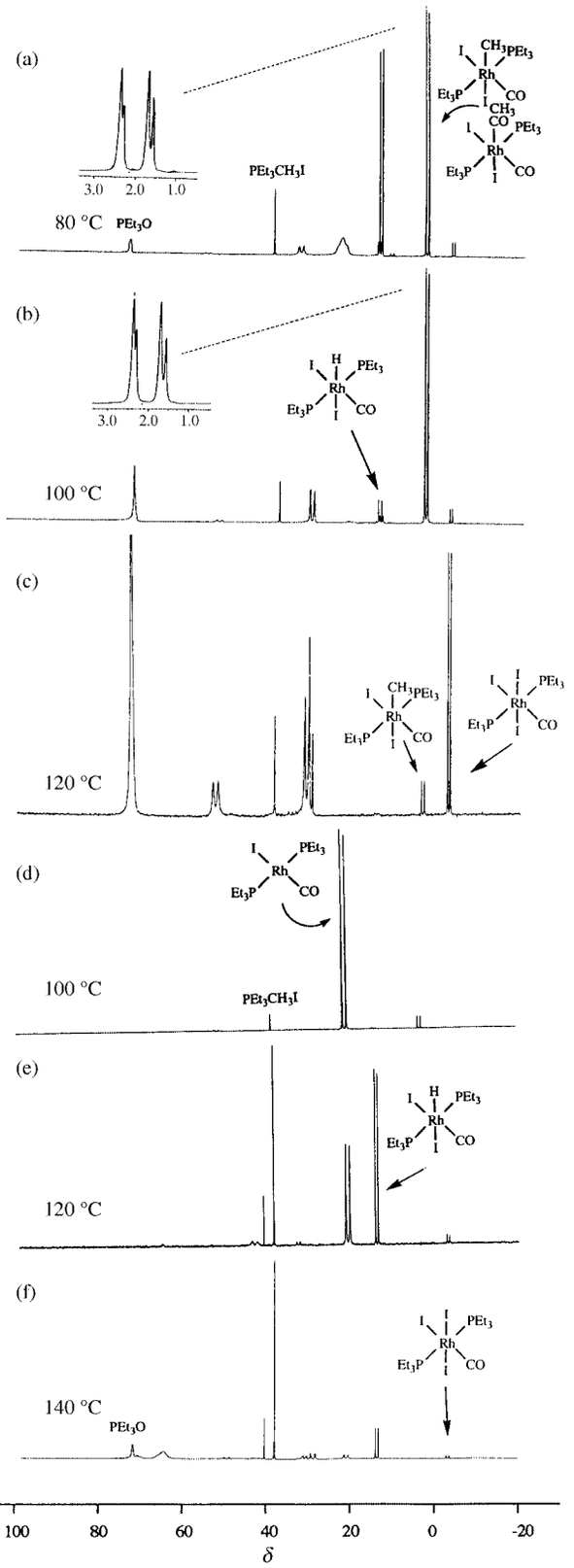

Fig. 12 ^{31}P NMR spectra, measured at 25 °C under argon, of solutions containing $[RhI(CO)(PEt_3)_2]$, and MeI that had been heated for 1 h under CO (40 bar). (a)–(c) in methanol, 80, 100, 120 °C, respectively; (d)–(f) in MeOAc, HOAc and water at 100, 120 and 140 °C, respectively.

$(PEt_3)_2]$ is the origin of the supposed monophosphine complexes and Et_3PO. This was confirmed by heating $[RhI_3(CO)(PEt_3)_2]$ in methanol containing water under CO (40 bar) at 120 °C for 1 h. The ^{31}P NMR spectrum showed that Et_3PO was the major product although small amounts of unreacted $[RhI_3(CO)(PEt_3)_2]$, a supposed monophosphine complex and $[RhI(CO)(PEt_3)_2]$ were also generated. In the absence of water, $[RhI_3(CO)(PEt_3)_2]$ was stable and Et_3PO was not produced.

These reactions suggest that the formation of $[RhI(CO)(PEt_3)_2]$, the loss of PEt_3 from $[RhI_3(CO)(PEt_3)_2]$ and the formation of Et_3PO only occur if water is present. The formation of $[RhI(CO)(PEt_3)_2]$ presumably occurs *via* water–gas shift type chemistry, whilst we propose that the formation of Et_3PO may occur through the reductive elimination of Et_3PI^+ and subsequent hydrolysis. In the absence of water, this reaction lies to the Rh^{III} side. These reactions are summarised in Scheme 5. The reverse reaction involving the oxidative addition of the P–I bond in R_3PI_2 to a variety of transition elements[44] or their complexes[45] has been documented.

One interesting implication of these results is that the rhodium triethylphosphine complexes are not intrinsically unstable towards dissociation of PEt_3 since if this were the case the major phosphorous containing decomposition product should be $[Et_3PMe]I$. Small amounts of this compound are formed but the relative amount does not correlate with the extent of catalyst degradation.

The catalytic studies described above suggested that water increased the activity of $[RhI(CO)(PEt_3)_2]$ as a catalyst for methanol carbonylation, as is also the case for $[RhI_2(CO)_2]^-$.[1] We, therefore, carried out analogous ^{31}P NMR studies on the catalytic reaction using methyl ethanoate, ethanoic acid, water and methyl iodide as the reaction medium again cooling the solution after 1 h and measuring the ^{31}P NMR spectra at ambient temperature under argon. Although the species produced are essentially the same as in the absence of added water, the catalyst degradation is much less. Even after heating at 140 °C little $[RhI_3(CO)(PEt_3)_2]$ or Et_3PO were produced [Fig. 12(d)–(f)].§ After heating at 120 °C and cooling, large amounts of $[RhHI_2(CO)(PEt_3)_2]$ are present but these do not lead on to $[RhI_3(CO)(PEt_3)_2]$ suggesting that the main reason for the increased catalyst stability arises because the HI is hydrated and is less available for reaction of $[RhHI_2(CO)(PEt_3)_2]$ to give $[RhI_3(CO)(PEt_3)_2]$. The presence of larger amounts of $[Et_3PMe]I$ and $[Et_3PH]I$ (δ 40.0) suggest that phosphine loss may occur in these systems by reductive elimination from $[RhXI_2(CO)(PEt_3)_2]$, X = H or Me (Scheme 5).

Interestingly, in the presence of water, $[RhI(CO)(PEt_3)_2]$ is the major species observed after heating at 100 °C consistent with MeI oxidative addition being rate determining as indicated by studies of catalytic reactions carried out in the presence of water.

X-Ray structure of $[RhMeI_2(CO)(PEt_3)_2]$

The X-ray crystal and molecular structure of $[RhMeI_2(CO)(PEt_3)_2]$ is shown in Fig. 5, with bond lengths and angles in Table 6. It confirms the mutually *trans* PEt_3 ligands and that the methyl group is *trans* to I. The methyl and carbon monoxide ligands are situated *cis* to one another, which is required for the migratory insertion step in the catalytic cycle.

There have been no previously published crystallographic analyses of complexes of the type, $[RhMeX_2(CO)(PR_3)_2]$ (X = halide, R = organic group). However, there are examples of crystal structures of other six-coordinate rhodium phosphine complexes where iodomethane has been oxidatively added.[46,47] These structures possess Rh–Me bond lengths of between 2.08 and 2.11 Å. Thus, the Rh–Me bond length in $[RhMeI_2(CO)(PEt_3)_2]$ (2.109 Å) is typical for a rhodium(III) methyl complex containing phosphine ligands. $[RhMeI\{C(N_2)SiMe_3\}(PMe_3)_3]$ exhibits similar Rh–I, Rh–Me and Rh–P bond lengths to $[RhMeI_2(CO)(PEt_3)_2]$.[48] Rhodium(III) complexes with the methyl and iodide ligands situated mutually

§ Although water is not added to these solutions, it will be generated as a reaction product by the overall reaction: 2 MeOH + CO ⟶ $MeCO_2Me + H_2O$

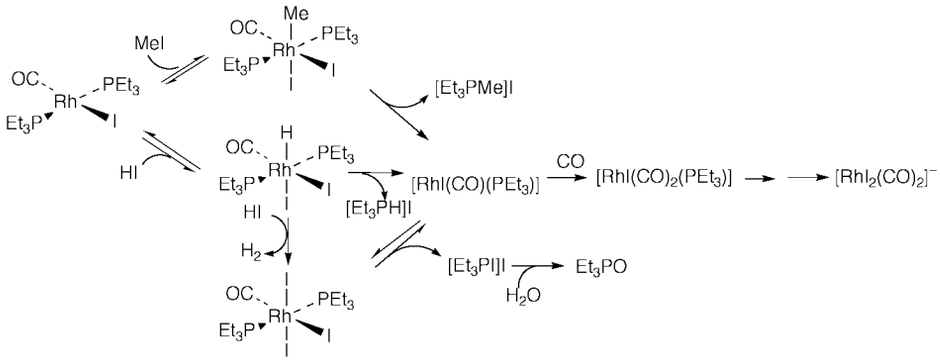

Scheme 5 Reactions leading to the deactivation of $[RhI(CO)(PEt_3)_2]$ during the catalytic carbonylation of methanol.

Table 6 Bond lengths (Å) and selected angles (°) for $[RhMeI_2(CO)(PEt_3)_2]$

I(1)–Rh(1)	2.7823(7)	I(2)–Rh(1)	2.721(1)
Rh(1)–P(1)	2.387(2)	Rh(1)–P(2)	2.390(2)
Rh(1)–C(1)	1.836(9)	Rh(1)–C(2)	2.109(9)
P(1)–C(3)	1.823(9)	P(1)–C(5)	1.839(9)
P(1)–C(7)	1.828(8)	P(2)–C(9)	1.832(8)
P(2)–C(11)	1.839(8)	P(2)–C(13)	1.826(8)
O(1)–C(1)	1.113(10)	C(3)–C(4)	1.52(1)
C(5)–C(6)	1.52(1)	C(7)–C(8)	1.51(1)
C(9)–C(10)	1.51(1)	C(11)–C(12)	1.52(1)
C(13)–C(14)	1.51(1)		
C–H	0.95[a]		
I(1)–Rh(1)–I(2)	94.18(4)	I(1)–Rh(1)–P(1)	90.34(5)
I(1)–Rh(1)–P(2)	91.36(5)	I(1)–Rh(1)–C(1)	89.0(2)
I(1)–Rh(1)–C(2)	173.8(2)	I(2)–Rh(1)–P(1)	89.48(5)
I(2)–Rh(1)–P(2)	88.22(5)	I(2)–Rh(1)–C(1)	176.3(2)
I(2)–Rh(1)–C(2)	91.8(2)	P(1)–Rh(1)–P(2)	177.24(7)
P(1)–Rh(1)–C(1)	92.2(3)	P(1)–Rh(1)–C(2)	88.1(2)
P(2)–Rh(1)–C(1)	90.0(3)	P(2)–Rh(1)–C(2)	90.4(2)
C(1)–Rh(1)–C(2)	85.0(3)	Rh(1)–P(1)–C(3)	112.5(3)
Rh(1)–P(1)–C(5)	113.2(3)	Rh(1)–P(1)–C(7)	119.2(3)
C(3)–P(1)–C(5)	103.2(4)	C(3)–P(1)–C(7)	101.7(4)
C(5)–P(1)–C(7)	105.2(4)	Rh(1)–P(2)–C(9)	114.9(3)
Rh(1)–P(2)–C(11)	117.3(3)	Rh(1)–P(2)–C(13)	114.7(3)
C(9)–P(2)–C(11)	98.1(4)	C(9)–P(2)–C(13)	104.4(4)
C(11)–P(2)–C(13)	105.4(4)	Rh(1)–C(1)–O(1)	175.8(8)
P(1)–C(3)–C(4)	115.2(6)	P(1)–C(5)–C(6)	116.5(7)
P(1)–C(7)–C(8)	117.6(7)	P(2)–C(9)–C(10)	116.0(6)
P(2)–C(11)–C(12)	117.5(6)	P(2)–C(13)–C(14)	117.1(6)

[a] Fixed value.

trans have the Rh–I bond lengths typically in the region 2.76–2.80 Å.[49,50] Thus, the Rh–I(1) bond length in $[RhMeI_2(CO)(PEt_3)_2]$ (2.7823 Å) is as expected for a rhodium(III) complex containing mutually *trans* methyl and iodide ligands.

Conclusions

Neutral rhodium complexes containing trialkylphosphines, *e.g.* $[RhI(CO)(PEt_3)_2]$ show higher activity for methanol carbonylation at 150 °C than the industry standard, $[RhI_2(CO)_2]^-$, in the presence of high concentrations of water. They degrade, however, to $[RhI_2(CO)_2]^-$ during the reaction. Detailed NMR and IR studies show that the rate of oxidation addition of MeI to the rhodium(I) centre is increased by a factor of 57 times at 25 °C whilst the insertion of CO into the Rh–C band is slowed by a factor of 38 times for the PEt_3 complexes than for the anionic complexes. Nevertheless, at least in water, oxidative addition is rate determining. There is some evidence that when starting with dry methanol¶ reductive elimination of ethanoyl iodide may become rate determining. The degradation of $[RhI(CO)(PEt_3)_2]$ to $[RhI_2(CO)_2]^-$ proceeds *via* $[RhHI_2(CO)(PEt_3)_2]$ and $[RhI_3(CO)(PEt_3)_2]$, from which reductive elimination of $[Et_3PI]^+$ leads to Et_3PO. In the presence of a large excess of water, $[RhI_3(CO)(PEt_3)_2]$ formation is surpressed, but Et_3P is lost, albeit much more slowly and at higher temperatures as $[Et_3PX]^+$ (X = Me or H).

¶ Water is generated during the reaction, so this is really a reaction carried out at low water concentration.

Acknowledgements

We thank BP Chemicals and the EPSRC for a studentship (J. R.) and the CEC through its TEMPUS programme for funding (A. C. B.). We are also indebted to Dr A. Haynes, Sheffield University, for many helpful discussions.

References

1 M. J. Howard, M. D. Jones, M. S. Roberts and S. A. Taylor, *Catal. Today*, 1993, **18**, 325.
2 C. S. Garland, M. F. Giles and J. G. Sunley, *Eur. Pat.*, 643 034, 1995; *Chem. Abstr.*, 1995, **123**, 86573g.
3 D. Forster, *Adv. Organomet. Chem.*, 1979, **17**, 255.
4 P. M. Maitlis, A. Haynes, G. J. Sunley and M. J. Howard, *J. Chem. Soc.*, *Dalton Trans.*, 1996, 2187 and references therein.
5 J. K. MacDougall, M. C. Simpson, M. J. Green and D. J. Cole-Hamilton, *J. Chem. Soc.*, *Dalton Trans.*, 1996, 1161.
6 M. C. Simpson, A. W. S. Currie, J. M. Andersen, D. J. Cole-Hamilton and M. J. Green, *J. Chem. Soc.*, *Dalton Trans.*, 1996, 1793.
7 W. Weston and D. J. Cole-Hamilton, *Inorg. Chim. Acta.*, 1998, **280**, 99.
8 M. J. Payne and D. J. Cole-Hamilton, *J. Chem. Soc.*, *Dalton Trans.*, 1997, 3167.
9 M. C. Simpson and D. J. Cole-Hamilton, *Coord. Chem. Rev.*, 1996, **155**, 163.
10 J. Chatt and B. L. Shaw, *J. Chem. Soc. A*, 1966, 1437.
11 F. E. Paulik, A. Hershman, W. R. Knox and J. F. Roth, *US Pat.*, 4 690 912, 1987; *Chem. Abstr.*, 1988, **108**, 7893a.
12 D. Brodski, C. Leclere, B. Denise and G. Pannetier, *Bull. Soc. Chim. Fr.*, 1976, **1**–**2**, 61.
13 M. J. Baker, J. R. Dilworth, J. G. Sunley and N. Wheatley, *Eur. Pat.*, 632 006, 1995; *Chem. Abstr.*, 1995, **122**, 164060h.
14 M. J. Baker, M. F. Giles, A. G. Orpen, M. J. Taylor and R. J. Watt, *J. Chem. Soc.*, *Chem. Commun.*, 1995, 197.
15 J. Freiberg, A. Weigt and H. Dilcher, *J. Prakt. Chem.*, 1993, **335**, 337; *Chem. Abstr.*, 1993, **119**, 226074q.
16 J. R. Dilworth, J. R. Miller, M. J. Baker and J. G. Sunley, *J. Chem. Soc.*, *Chem. Commun.*, 1995, 1579.
17 C. M. Bartish, *US Pat.*, 4 102 920, 1978; *Chem. Abstr.*, 1978, **89**, 163081d.
18 R. W. Wegman, A. G. Abatjoglou and A. M. Harrison, *J. Chem. Soc.*, *Chem. Commun.*, 1987, 1891.
19 R. W. Wegman and D. J. Schreck, *US Pat.*, 5 026 907, 1991; *Chem. Abstr.*, 1991, **115**, 184551c.
20 R. W. Wegman and A. G. Abatjoglou, *PCT Int. Appl. WO*, 8 600 888, 1986; *Chem Abstr.*, 1986, **105**, 174788q.
21 R. W. Wegman, *Eur. Pat.*, 171 804, 1986; *Chem. Abstr.*, 1986, **105**, 78526g.
22 R. W. Wegman and D. J. Schreck, *Eur. Pat.*, 173 170, 1986; *Chem. Abstr.*, 1986, **105**, 78523d.

23 R. G. Cavell and K. V. Katti, *Can. Pat.*, 2 024 284, 1992; *Chem. Abstr.*, 1992, **117**, 251564r.
24 R. G. Cavell and K. V. Katti, *US Pat.*, 5 352 813, 1994; *Chem. Abstr.*, 1995, **122**, 31417m.
25 E. Lindner and E. Glaser, *J. Organomet. Chem.*, 1990, **391**, C37.
26 S. Bischoff, A. Weigt, J. Freiberg, H. Miessner and B. Lucke, *9th International Symposium on Homogeneous Catalysis*, Jerusalem, 1994.
27 S. Bischoff, A. Weigt, H. Miessner and B. Lucke, *Energy Fuels*, 1996, **10**, 520.
28 S. Bischoff, A. Weigt, H. Miebner and B. Lucke, *Prepr. Pap - Am. Chem. Soc., Div. Fuel Chem.*, 1995, **40**, 114.
29 A. Bader and E. Lindner, *Coord. Chem. Rev.*, 1991, **108**, 27.
30 J. Rankin, A. D. Poole, A. C. Benyei and D. J. Cole-Hamilton, *Chem. Commun.*, 1997, 1835.
31 G. W. Parshall, *Inorganic Synthesis*, McGraw-Hill, New York, 1972, p. 90.
32 A. Fulford, C. E. Hickey and P. M. Maitlis, *J. Organomet. Chem.*, 1990, **398**, 311.
33 SIR 92: A. Altomare, G. Cascarano, G. Giacovazzo and A. Guagliardi, *J. Appl. Crystallogr.*, 1994, **27**, 1045; A. Altomare, C. Giacovazzo and A. Moltierni, *Acta. Crystallogr. Sect. A*, 1994, **50**, 585.
34 D. T. Cromer and J. T. Cromer, in *International Tables for X-Ray Crystallography*, Kynoch Press, Birmingham, 1974, vol 4, Table 2.2A.
35 TEXSAN, Crystal Structure Analysis Package, Molecular Structure Corporation, Houston, TX, 1985 and 1992.
36 I. C. Douek and G. Wilkinson, *J. Chem. Soc. A*, 1966, 2604.
37 S. Franks, F. R. Hartley and J. R. Chipperfield, *Inorg. Chem.*, 1981, **20**, 3238.
38 R. F. Heck, *J. Am. Chem. Soc.*, 1964, **86**, 2796.
39 S. Franks, F. R. Hartley and J. R. Chipperfield, *Adv. Chem.*, 1982, **196**, 273.
40 D. Forster, *J. Am. Chem. Soc.*, 1975, **97**, 951.
41 R. C. Gash, D. J. Cole-Hamilton, R. Whyman, J. C. Barmes and M. C. Simpson, *J. Chem. Soc., Dalton Trans.*, 1994, 1963.
42 A. Haynes, B. E. Mann, G. E. Morris and P. M. Maitlis, *J. Am. Chem. Soc.*, 1993, **115**, 4093; P. R. Ellis, J. M. Pearson, A. Haynes, H. Adams, N. A. Bailey and P. M. Maitlis, *Organometallics*, 1994, **13**, 3215.
43 J. Ramsey and J. Ladd, *J. Chem. Soc.*, 1968, 188.
44 P. T. Ndiform, C. A. McAuliffe, A. G. Mackie and R. G. Pritchard, *Inorg Chim. Acta.*, 1998, **282**, 25 and references therein.
45 H. P. Lane, S. M. Godfrey and C. A. McAuliffe, *Inorg. Chim. Acta*, 1996, **247**, 257.
46 M. Cano, J. V. Heras, M. A. Lobo, E. Pinilla and M. A. Monge, *Polyhedron*, 1992, **11**, 2679.
47 S. S. Basson, J. G. Leipoldt, A. Roodt and J. A. Venter, *Inorg. Chim. Acta*, 1987, **128**, 31.
48 M. J. Menu, P. Desrosiers, M. Dartiguenave and Y. Dartiguenave, *Organometallics*, 1987, **6**, 1822.
49 T. G. Schenck, C. R. C. Milne, J. F. Sawyer and B. Bosnich, *Inorg. Chem.*, 1985, **24**, 2338.
50 G. J. Lamprecht, G. J. Van Zyl and J. G. Leipoldt, *Inorg. Chim. Acta*, 1989, **164**, 69.
51 A. Haynes and L. Gonsalvi, personal communication.

Paper 9/05308E